Plasma Chemistry and Plasma Processing (2021) 41:841–854
https://doi.org/10.1007/s11090-021-10155-w

ORIGINAL PAPER

Rapid Atmospheric Pressure Ambient Air Plasma Functionalization of Poly(styrene) and Poly(ethersulfone) Foils

Július Vida[1] · **Martina Ilčíková**[1] · **Roman Přibyl**[1] · **Tomáš Homola**[1]

Received: 29 April 2020 / Accepted: 24 December 2020 / Published online: 25 February 2021

Abstract
Activation of polymeric surfaces, i.e. formation and/or modification of the functional groups on the surface of a material, is essential prior to the further processing of polymers, especially in applications where wettability plays a crucial role. In this study, an atmospheric pressure ambient air plasma treatment of poly(styrene) (PS) and poly(ethersulfone) (PES) foils using diffuse coplanar surface barrier discharge is presented. The plasma treatment for 0.5 s resulted in a decrease of water contact angle from the original value of 83° to 26° for PS and from 76° to 32° for PES. No significant changes in wettability were observed for prolonged treatment times. Better wettability was correlated with decreasing carbon to oxygen ratio resulting from an incorporation of oxygen-containing functional groups C–OH, C=O and O–C=O on the surface. X-ray photoelectron spectroscopy was employed to study details in the changes of the surface chemistry following the plasma exposure. We used atomic force microscopy to study the formation of low molecular weight oxidized material (LMWOM) during the plasma treatment. After dissolving the LMWOM in water, we observed roughening of the plasma-treated surfaces at the nanometre level due to etching induced by plasma treatment.

Keywords Ambient air plasma treatment · DCSBD · Flexible foils · Polyethersulfone (PES) · Polystyrene (PS) · LMWOM

Introduction

Polymers are ubiquitous in industrial and scientific applications and are generally among the most widely used materials. The reason is their versatility and durability combined with rather low price and weight. The bulk and the surface properties of polymers depend on the type of the material. Pristine polymers often have low surface energy, resulting in hydrophobic nature of their surface [1, 2]. This suggests that polymers typically require bulk or surface modifications prior to specific applications to achieve desirable properties [3–6].

✉ Július Vida
jvida@mail.muni.cz

[1] Department of Physical Electronics, Faculty of Science, Masaryk University, Kotlářská 267/2, 611 37 Brno, Czech Republic

For instance, poly(ethersulfone) (PES) is a promising material for medical applications and waste-treatment membranes providing good properties in wide range of environments [7, 8]. The biggest disadvantage, and the limitation of PES, arises from the hydrophobicity of its surface, which makes the membranes prone to fouling by an adsorption of nonpolar solutes, hydrophobic particles or biofilm [9]. The fouling of membranes for water purification reduces the filtration capabilities, thus shortening their lifespan and increasing the operational costs [10–12]. Another emerging field for the application of polymers is microfluidic devices. Microfluidics are capable of highly sensitive, fast, high-throughput and low-cost analysis by manipulation of a fluid using micro-structured channels and chambers [13]. Various thermoplastics can be used to fabricate microfluidic chips, including poly(styrene) (PS) [14, 15]. The natural hydrophobicity of PS renders the handling of the fluids in microfluidic devices problematic [16].

The hydrophobicity and low wettability are linked to the low surface energy of a material. For hydrophilization of a polymer, the polar component of the surface energy should be introduced. Increasing the hydrophilicity of a polymer can be realized by chemical altering of the bulk properties [17]. On the other hand, surface treatment is faster and simpler process for alteration of the surface properties. Numerous techniques have been studied and practically applied, however, plasma treatment is usually used for tailoring the surface properties and enhancing wettability of polymers [18–23]. Plasma-processing achieves a high quality of the resulting treatment and represents an environmentally-friendly alternative over the wet chemical treatment [1]. Oxygen-containing plasma treatment can induce functional groups on the treated surface, such as hydroxyls (C–OH), ethers (C–O–C), carbonyls (C=O) or carboxyls (O–C=O). The formation of the functional groups is a result of an interaction between energetic reactive species in plasma (electrons, excited and metastable atoms and molecules, positive and negative ions, etc.) with the treated surface. Functional groups containing oxygen increase the polar component of the surface energy, which leads to better wettability and adhesion [5, 19]. The same reactive species can lead to scission of polymer chains. The plasma-induced chain scission leads to formation of highly oxidized oligomers on the surface. These lighter species are often referred to as low molecular weight oxidized material (LMWOM). LMWOM can be removed from the surface by polar solvents such as water and are regarded as a form of degradation of the plasma-treated surface [24, 25]. Besides the functionalization, etching of the surface can occur during the plasma treatment. It can additionally influence the wettability changes as it increases the surface roughness and has been previously used for creating nanostructures on the surfaces of polymers [26, 27].

In this study we performed an atmospheric pressure plasma treatment of PES and PS (Fig. 1) foils in ambient air. Ambient air plasma at atmospheric pressure has the significant advantage as no expensive vacuum systems or additional working gases are required, rendering the operation simpler and cheaper compared to low-pressure plasmas. We used a proprietary dielectric barrier discharge (DBD) with a coplanar arrangement of electrodes: diffuse coplanar surface barrier discharge (DCSBD). The DCSBD generates a diffuse, macroscopically homogeneous and thin layer of plasma, as displayed in Fig. 2. It can produce plasma with very high power density up to 100 W cm^{-3} [2]. The thin layer in which the plasma is generated in DCSBD enables an efficient utilization of the full potential of the discharge, including charged species, radicals and UV radiation, unlike volume DBD setups where plasma is generated in a thicker volume between electrodes [28]. Furthermore, the generation of plasma on the surface of the dielectric eliminates any restrictions on the thickness of the treated sample. The filaments of the discharge propagate parallelly to the treated surface eliminating possible damage by pinhole effect [29]. It has proven

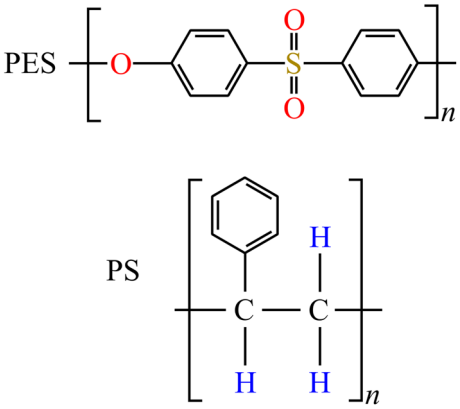

Fig. 1 Schematic structure of PES and PS polymers

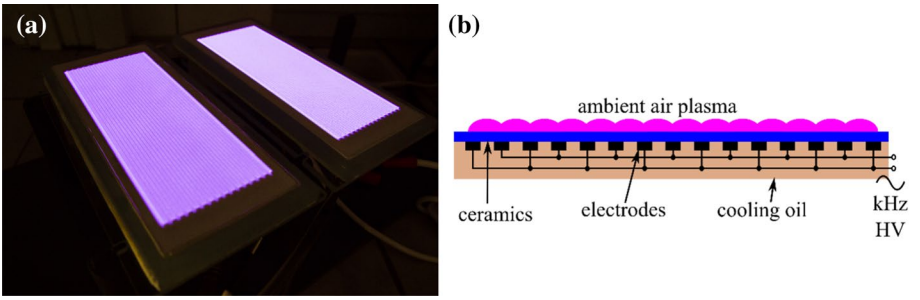

Fig. 2 Diffuse coplanar surface barrier discharge (DCSBD) **a** two plasma units operating at full power 400 W/plasma unit under ambient air conditions, **b** scheme of a cross section of the plasma unit

very effective for treatment of temperature-sensitive materials like polymers [30], as its operational temperature is around 70 °C. A great advantage of this system is the ability to treat large surfaces and its compatibility with roll-to-roll processing, which is highly desirable by the industry [31].

Experimental Section

Materials and Plasma Treatment

A transparent PES foil with thickness of 25 μm and transparent biaxial-oriented PS foil with a thickness of 125 μm were purchased from Goodfellow Cambridge Ltd. (United Kingdom). The supplier has labelled both foils as amorphous, which will be discussed further in the context of the plasma etching of the surface. The samples were cut into approximately 1 × 1 cm pieces.

The plasma treatment of the foils was performed by atmospheric-pressure ambient air plasma generated by diffuse coplanar surface barrier discharge (DCSBD), which was commercialized by Roplass s.r.o (Czech Republic), displayed in Fig. 2. DCSBD operated at continuous-wave AC with frequency of 15 kHz. It generates plasma with an area

of 160 cm^2 and a thickness about 0.3 mm. The total power in plasma was 400 W, i.e. the surface power density and the volume power density were approximately 2.5 W cm^{-2} and 83 W cm^{-3}, respectively [32]. The power dose can be calculated as an energy delivered to a unit of area during the treatment time [33, 34]. The treatment time varied between 0.5 and 16 s, i.e. power doses in the interval between 1.25 and 40.0 J cm^{-2}. The distance between the sample and the surface of the DCSBD unit was kept at 0.3 mm during the treatment, to ensure a contact with the diffuse part of the discharge. Furthermore, the holder onto which the samples were mounted was moving over the plasma region of DCSBD to ensure homogeneous plasma treatment.

Surface Analysis

The wettability of the PES and PS foils was evaluated by a measurement of the water contact angle (WCA) using SeeSystem (Advex Instruments, Czech Republic). Water droplet with volume of 1 µl was deposited onto the surface using a micropipette. The images of the droplets for analysis were taken approximately 3 s after the deposition. The average WCA was calculated from approximately 15 measurements.

The elemental composition and the surface bonding states were determined from XPS spectra obtained by AXIS Supra spectrometer (Kratos Analytical Ltd. United Kingdom). The instrument uses AlKα spectral line (1486.6 eV photon energy) and an electron flood gun was utilized for charge compensation. The acquisition of narrow regions of the spectrum was performed with the pass energy 20 eV. For analysis of the spectra CasaXPS software was used. The spectra were calibrated to C–C/C–H peak of C 1 s at 284.8 eV binding energy. The U Poly Tougaard background type was used and the components in the XPS spectra were fitted with a symmetrical mixed Gauss-Lorentzian lines. The measurement was performed on two spots for each sample and the data are presented with a relative uncertainty of 5%.

The surface roughness and the morphology of the surface were measured by AFM instrument Ntegra Prima (NT-MDT, Russia). The root mean square (RMS) roughness was determined from 5 × 5 µm scans with 512 dpi resolution and scanning rate between 0.5 and 0.7 Hz in semi-contact mode.

To study the degradation of the surfaces by LMWOM, the plasma-treated surfaces were washed in deionized water in ultrasonic bath for 5 min. It was shown by Strobel et al. [25] that even shorter washing is sufficient to remove most of the LMWOM. The selected rinsed samples were analysed by AFM.

Results and Discussion

Wettability

The results of wettability measurement by WCA analysis for PES are shown in Fig. 3a as a function of treatment time and power dose. The pristine PES displayed the WCA of 75° ± 2°. A significant decrease in WCA was observed after just a short treatment time of 0.5 s, after which the WCA dropped to 32° ± 5°. For PES, the effect of the plasma treatment became quickly saturated and prolonged exposure (higher power doses) lead to no further decrease of WCA. Similar effect of increased wettability was observed by other authors after plasma treatment of PES films [18, 20, 35] or membranes [36–38]

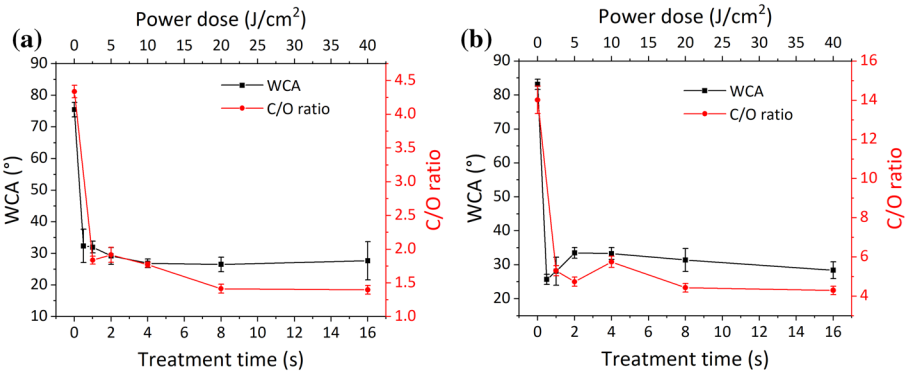

Fig. 3 Water contact angle (WCA) and C/O ratio of **a** PES and **b** PS foil as a function of plasma treatment time and power dose

with various types of atmospheric-pressure and low-pressure discharges, however, either treatment times in the order of minutes, use of noble gases or vacuum systems were required. Significantly shorter treatment times and the operation at ambient conditions is a huge benefit of this approach.

Ambient air plasma-treated PS foil displayed similar increase in wettability. In Fig. 3b the WCA rapidly dropped from $83° \pm 2°$ for untreated sample to $26° \pm 2°$ after 0.5 s treatment. Similar trend has been previously observed after cold oxygen plasma treatment in RF discharge at reduced pressure [39, 40]. Atmospheric pressure DBD [41] and plasma jet [42] were also tested for hydrophilization of PS surfaces, however, longer treatment times (minutes) were needed and the effect was local, therefore not suitable for large area processing. As can be observed in Fig. 3b, after the initial decrease of WCA, higher power dose results in slightly worse wettability and higher WCA, $34° \pm 2°$ after 2 s treatment. This effect was observed in the study of Bitar et al. [41] and was attributed to removal of the initially induced functional groups by reactions with plasma, until an equilibrium is reached between these two opposing effects.

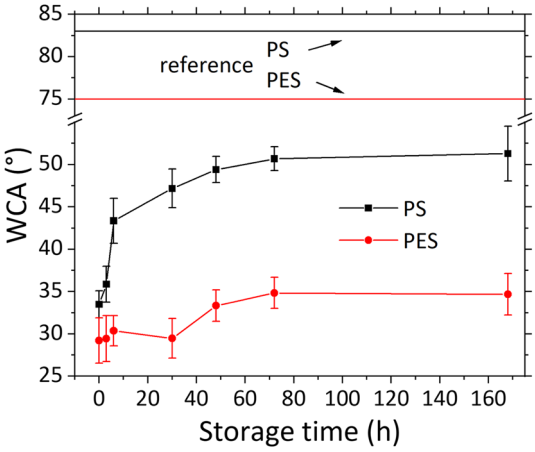

Fig. 4 Changes in the water contact angle (WCA) on the surface of PES and PS foil plasma-treated for 2 s after storing in ambient conditions for up to 170 h

To study the aging effect of plasma-treated surface of PES and PS foils, samples were treated for 2 s and stored in ambient conditions for up to 168 h. Results presented in Fig. 3 clearly demonstrate that after 2 s the effect of plasma treatment on the wettability of the surface is already saturated for PES as well as for PS. Changes in the wettability over time are presented in Fig. 4, where the WCA of PES and PS is shown as a function of storage time. The WCA of PS surface increased significantly after just six hours of storage from $34° \pm 2°$ to $43° \pm 3°$ and then saturated at $51° \pm 1°$ after approximately 72 h. The diminishing of the effect of plasma treatment of the surface of PES was less significant and the WCA saturated at $35° \pm 2°$ from the initial $29° \pm 3°$ after approximately 72 h of storage. The hydrophobic recovery of plasma-treated polymers depends on the treatment and storage condition [43] as well as on material properties like glass transition temperature [44] and the degree of crystallinity [45]. As both materials were treated and stored in the same conditions and they both had amorphous structure, the difference in glass transition temperature could be related to higher stability of plasma treatment of PES because it has higher glass transition temperature than PS.

Surface Chemistry

Elemental Composition

The surface chemistry and the changes in the surface chemistry of PES and PS foils induced by ambient air plasma treatment were studied by XPS. The elemental composition of the surface of polymers is summarized in Tables 1 and 2, for PES and PS, respectively. In Fig. 3 the carbon to oxygen (C/O) ratio is plotted as a function of plasma treatment time together with the WCA. The pristine PES and PS polymers exhibited C/O ratio of 4.3 and 14.0, respectively. After the 0.5 s treatment time the C/O ratio on the surface of both polymers dropped significantly to 1.8 and 5.3, for PES and PS respectively, and remained relatively stable with prolonged exposure to plasma. The common trend in the evolution of WCA and C/O ratio with prolonged treatment times indicates, that oxidation of the surface during the plasma exposure was a significant reason for the improved wettability of the surface.

PES has a chemical formula $(C_{12}H_8O_3S)_n$ and its structure (Fig. 1) consists of aromatic rings linked alternatively by ether and sulfone groups. The C/O and C/S ratios from Table 1 for pristine PES 4.3 and 18.0, respectively, are slightly higher than the expected ratios according to the chemical formula 4 and 12, respectively. This excess of carbon on the surface can be attributed to contamination on the polymer's surface. Interestingly, the concentration of sulfur on the surface decreases slightly over the duration of the plasma treatment, which was attributed by Feng et al. [20] to the loss of some readily-volatile sulfur-containing products during the plasma treatment. The ambient air plasma treatment resulted in incorporation of around 2% of nitrogen.

PS (Fig. 1) has a chemical formula $(C_8H_8)_n$ and thus only carbon was expected to be visible in the XPS spectrum. However, even the surface of pristine PS was contaminated by around 6.3% of oxygen, which can be explained by samples not being handled in ultra-clean environment. Traces of fluorine were present in the spectrum as well, although the signal was very low, and it disappeared completely after the plasma treatment. The surface also contained around 5% of silicon, which remained the same after plasma treatment, possibly a signal from a tape used to fix the samples on the holder.

Table 1 Elemental composition of the surface of the untreated and plasma-treated PES foil

Treatment time	C [%]	O [%]	S [%]	N [%]	C/O ratio	C/S ratio
0 s	77.8	17.9	4.3	0	4.3	18.0
1 s	60.9	33.1	4.2	1.8	1.8	14.6
2 s	61.7	32.2	4.2	1.9	1.9	14.7
4 s	60.4	34.1	3.7	1.8	1.8	16.5
8 s	55.5	39.2	3.5	1.8	1.4	15.8
16 s	55.0	39.4	3.4	2.2	1.4	16.1
Theoretical	75.0	18.75	6.25	0	4.0	12.0

Table 2 Elemental composition of the surface of the untreated and plasma-treated PS foil

Treatment time	C [%]	O [%]	N [%]	F [%]	Si [%]	C/O ratio
0 s	88.9	6.3	0.0	0.4	4.4	14.0
1 s	78.8	14.9	0.9	0	5.4	5.3
2 s	77.6	16.4	1.2	0	4.8	4.7
4 s	80.0	13.9	0.8	0	5.3	5.8
8 s	75.7	17.1	1.5	0	5.7	4.4
16 s	75.5	17.6	1.1	0	5.8	4.3
Theoretical	100.0	0	0	0	0	∞

Surface Functionalization

Figure 5a shows the narrow region of C 1s in the XPS spectra of PES. The C 1s peak consisted of a main peak at 284.8 eV binding energy, corresponding to C–C/C–H bonds in the phenyl groups of PES, a peak at approximately 286.5 eV, representing the ether groups of PES, two peaks at around 287.3 and 288.8 eV binding energy corresponding to C=O and O–C=O groups, respectively, and a $\pi \rightarrow \pi^*$ shake-up satellite peak at around 291.6 eV, associated with the aromatic rings [20, 35]. It is a known problem of sulfur-containing

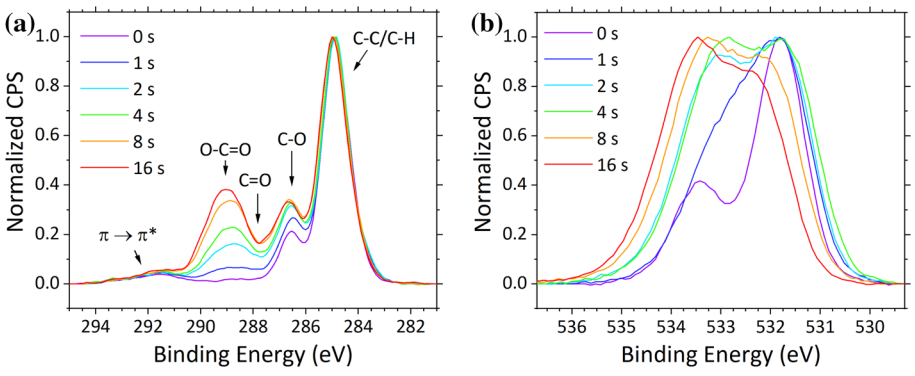

Fig. 5 Changes in the structure of the **a** C 1 s and **b** O1s peaks in the XPS spectra of PES induced by the ambient air plasma treatment for different duration

polymers, that the C–S peak occurs at a similar binding energy as the C–C/C–H component, around 285.3 eV [20], and is therefore difficult to distinguish in the XPS spectrum. The deconvolution of the C 1s peak shown in Fig. 5a was therefore performed using only five synthetic components mention above, as the C–S components was not well pronounced. The shares of the individual components can be followed in Table 3. The pristine PES consists mostly of two components, C–C/C–H and C–O–C, in a ratio of 6.8 to 1, which is higher than the expected ratio of 6 to 1, given by the structure of PES monomer. This discrepancy is caused by signal from C–S bonds contributing to the overall intensity of the C–C/C–H component. The relative intensity of the C=O and O–C=O components was below 2%. With increasing plasma treatment time, we observed a significant growth of the signal representing the carboxyl O–C=O component to 7.0% after 1 s and up to 27.6% after 16 s. Simultaneously, the relative intensity of the C–C/C–H component reduced by 28.6% after 16 s treatment. The increase in the signal from the C=O component were 1.1% after 16 s, and the C–O–C component remained almost unchanged.

It was suggested by Gonzalez and Hicks [22] and Gonzalez et al. [35] that oxidation of PES surface by oxygen plasma results in formation of carboxylic acid. This is in accordance with the results presented here. Similar behavior was also observed by other authors [18] after treatment of PES in RF inductively coupled oxygen plasma at reduced pressure. In their case, the relative intensity of the O–C=O component became quickly saturated and did not increase with prolonged exposure to plasma. The difference in our results can be possibly explained by gradual increase of the effective surface area resulting from the roughening of the surface. This will be discussed in the following section.

The narrow region of O 1s transition in the XPS spectrum of PES is shown in Fig. 5b. The untreated sample displays two peaks at 531.6 and 533.3 eV binding energy, corresponding to the oxygen bound to sulfur in O=S and oxygen bound to carbon in O–C–O, respectively [46]. They are in a ratio of roughly 2 to 1, which corresponds well with the structure of PES. After the plasma treatment the peak at the higher binding energy increases significantly. This is related to the appearance of carboxyl functional groups on the surface. Similar results were obtained by other authors after oxygen plasma treatment of PES [35].

Similarly, the narrow region of C 1s of PS foil was studied and the changes in its structure with progressively longer plasma treatment are displayed in Fig. 6a. The evolution of the shares of individual components can be followed in Table 3. The untreated surface of PS consisted of a slightly asymmetrical peak composed 91.8% of C–C/C–H component at 284.8 eV binding energy and 5.9% of C–O/C–OH component around 1.5 eV towards

Table 3 Evolution of the shares of individual components of the C 1 s peak in the XPS spectrum of PES and PS foils

Treatment time	C–C/C–H [%]		C–O–C/C–OH [%]		C=O [%]		O–C=O [%]	
	PES	PS	PES	PS	PES	PS	PES	PS
0 s	84.5	91.8	12.4	5.9	1.6	1.6	1.5	0.7
1 s	76.2	79.0	13.4	12.0	3.4	5.4	7.0	3.6
2 s	70.9	79.9	14.1	10.8	3.1	6.0	11.8	3.3
4 s	63.7	83.8	13.0	8.0	4.3	5.3	19.0	2.9
8 s	56.7	80.2	12.8	10.0	2.3	6.0	28.1	3.8
16 s	55.9	80.3	12.4	9.2	2.7	6.6	27.6	3.9

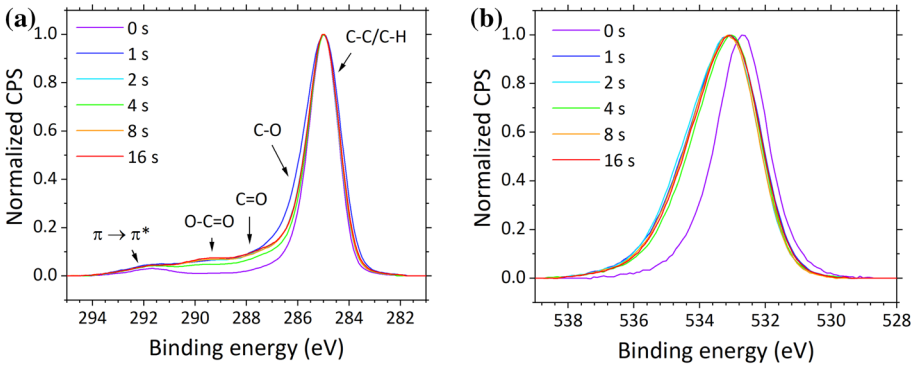

Fig. 6 Changes in the structure of the **a** C 1 s and **b** O1s peaks in the XPS spectra of PS induced by the ambient air plasma treatment for different duration

higher binding energies. A small intensity, bellow 2% of C=O and O–C=O components at 3 and 4 eV towards higher binding energies was attributed to surface contamination. A satellite peak from $\pi \rightarrow \pi^*$ shake-up at around 291.6 eV was also visible. With longer plasma exposure the C=O and O–C=O components increased from 1.6 and 0.7 to 5.4 and 3.4% after 1 s and remained at stable intensities for longer treatment times. This was a result of oxidation of the surface and was consistent with findings of other authors [39–41]. Interestingly, the relative intensity of the C–O/C–OH component initially grew after 1 s treatment and then decreased slightly with longer treatment times. This finding brings together the wettability results with the XPS results, where the slight increase of WCA for exposure longer than 1 s was ascribed to the removal of the initially induced polar functional groups by reactions with plasma.

Compared to the gradual increase in the intensities of the oxygen-containing functional groups that was observed for PES surface with prolonged plasma treatment, the shape of C 1s peak of PS remained relatively unchanged with treatment times longer than 1 s. This can be possibly explained by a slower, or more uniform etching of the surface of PS compared to PES and therefore unchanged effective surface area of the surface of PS. This will be discussed further in the context of the changes in the morphology of the surface in the following section. The narrow region of O 1s showed in Fig. 6b displayed a broadening of the initial peak as well as a shift towards higher binding energies caused by an increased amount of O–C=O and O–C–OH, which is consistent with the results of PES treatment and a treatment of different polymers with the same DCSBD discharge [30].

Structure and Morphology of the Surface

Plasma treatment of the surfaces of materials, including polymers, can influence the morphology of the treated surface. AFM was employed to study the changes in the morphology induced by the removal of material in an etching process, which roughens the surface of the polymer. Plasma treatment of polymers is also known to cause chain scission and formation of low-molecular weight oxidized material (LMWOM) [25]. LMWOM also causes surface roughening manifested by “bumps” on the surface.

In Fig. 7 are shown images of AFM scans of untreated and ambient air plasma-treated PES and PS samples. The untreated samples displayed very smooth surfaces with RMS

Table 4 RMS roughness of untreated and plasma treated PES and PS foils evaluated from AFM measurement

Treatment time	PES RMS roughness [nm]	PS RMS roughness [nm]
0 s	1	2
1 s	3	1
16 s	49	1
16 s (washed)	4	1

roughness of 1 nm and 2 nm, respectively (Table 4). The treatment of PES resulted in a visibly increased roughness of the surface to 3 nm and 49 nm after 1 s and 16 s plasma treatment, respectively. In Fig. (7b, c) a peaky structure that formed on the surface of PES can be seen. Oppositely, PS samples treated by plasma (Fig. 7e–f) showed no significant change in the roughness of the sample or the surface morphology. The increasing surface roughness that was observed for PES and not for PS can also explain the different trend in the changes of the structure of C 1s peak in Figs. 5a and 6a. Increasing surface area associated with higher roughness probably caused the gradual increase in the intensity of oxygen-containing functional groups. This was not observed for PS, where the surface was saturated by functional groups after initial treatment and because of stable surface area the intensity in XPS spectra did not increase further.

Thanks to the homogeneous plasma treatment, the etching effect should be also homogeneous over the whole surface of the sample. However, previous studies have shown, that the degree of crystallinity of the polymer affects the homogeneity of the etching. Plasma treatment of semi-crystalline poly(ethylene terephthalate) has shown a faster etching of the amorphous parts compared to the crystalline, creating a surface with a ordered peaky

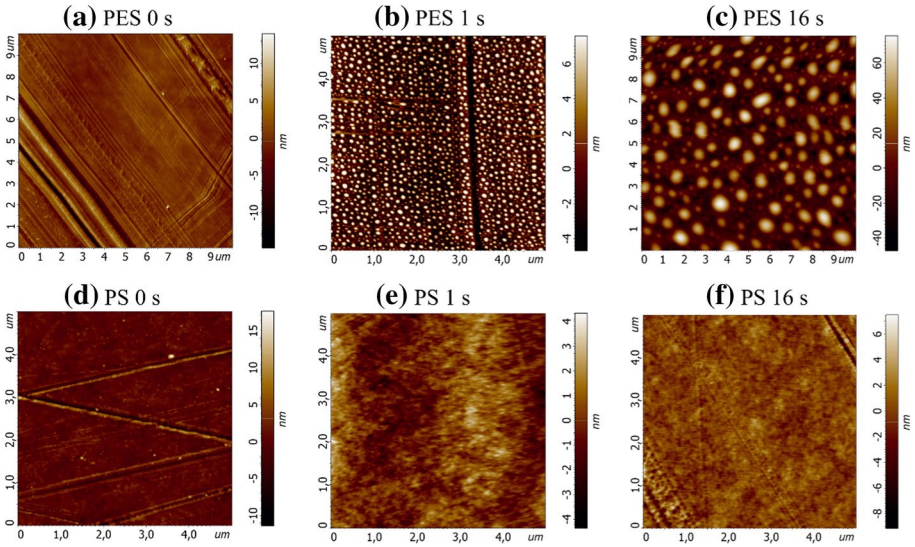

Fig. 7 AFM images displaying the morphological changes induced by the ambient air atmospheric pressure plasma on the surface of **a**–**c** PES and **d**–**f** PS foils. PES surface treated for 16 s in **c** is displayed in larger 10×10 μm^2 image to better showcase the size of the bumpy structure

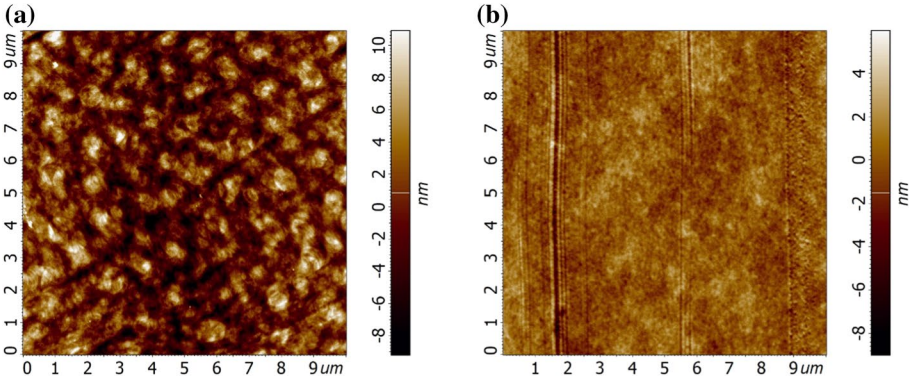

Fig. 8 AFM scan of the 16 s plasma-treated surface of **a** PES and **b** PS after washing in water

structure [19, 47]. On the other hand, plasma treatment of amorphous PET resulted in more homogeneous etching and smaller changes in the roughness of the surface [48]. Both PES and PS foils used were amorphous, thus the structure that was formed on the surface of PES cannot be a result of non-uniform etching. It seems that the degradation of the surface by chain scission and formation of LMWOM on the surface could explain the difference between PES and PS surfaces.

To verify, PES and PS samples treated in plasma for 16 s and subsequently washed in water were analysed by AFM. Figure 8 shows the AFM scan for the washed 16 s plasma-treated surfaces. We clearly see the removal of the bumps that formed on PES after plasma treatment shown in Fig. 7c. The water dissolved the LMWOM from the surface which resulted in the lower RMS roughness around 4 nm (Table 4). 2D AFM profiles shown in Fig. 9 indicate that the smooth bumps were removed from the surface. However, comparison with the reference sample showed that the roughness increased and some trenches were formed on the surface, which coud be attributed to plasma etching. Material that was removed from these places on the surface might have been the source of the LMWOM that

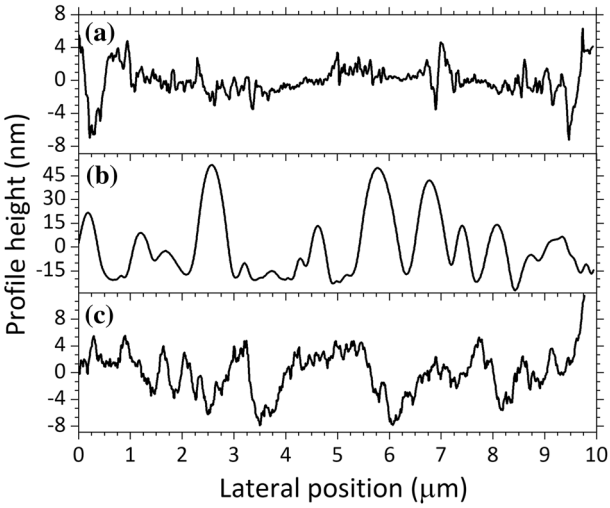

Fig. 9 2D AFM scans comparing the profiles of the **a** reference, **b** 16 s plasma-treated and **c** 16 s plasma-treated and washed PES surface

agglomerated in the bumps on the surface and was later washed away by water. The structure of the surface of PS after washing in Fig. 8b did not change compared to the surface prior to washing in Fig. 7f. This correlates with the stable RMS roughness of the surface of PS during plasma treatment, which suggests either more uniform formation of LMWOM or no formation of LMWOM during plasma treatment.

Conclusion

In this work, atmospheric pressure ambient air plasma treatment was performed on poly(ethersulfone) and poly(styrene) polymer foils. The results presented in this work show that rapid (0.5 s) surface treatment by the DCSBD leads to an improved wetting of the surface, with longer treatment times having little or no effect on further improvement of the hydrophilicity of the surface. The XPS analysis and deconvolution of the C 1s peaks showed that rapid functionalization of the surface is responsible for the increased hydrophilicity. The decreased water contact angle was directly correlated with a carbon to oxygen ratio, which was set as an good indicator of the functionalization of the surface as the C=O and O–C=O functional groups created during the oxidation of the surface are responsible for increase in the surface energy of the studied polymers. The plasma treatment resulted in formation of low molecular weight oxidized material on the surface. Washing of the plasma-treated surfaces with water resulted in dissolving of LMWOM. While on PES AFM revealed that ordered bumps with high RMS roughness formed, suggesting agglomeration of the LMWOM, on PS the effect of plasma was more uniform, and the roughness did not increase after treatment. The agglomeration of the LMWOM into bumpy structure on the surface of PES led to a gradual increase of the relative intensity of the oxygen-containing functional groups with longer plasma exposure detected in the narrow XPS region of C 1s. The surface of the PS, where the agglomeration was not observed was quickly saturated with oxygen-containing functional groups and their intensity in the XPS spectra did not increase further. After dissolving the LMWOM by washing in water an etching effect on the nanometer scale was observed, which could also have an effect on the wettability of the surfaces.

Acknowledgements This research has been supported by projects LM2018097 and LM2018110 funded by Ministry of Education, Youth and Sports of Czech Republic.

References

1. Vesel A, Mozetic M (2017) J Phys D Appl Phys 50(29):293001. https://doi.org/10.1088/1361-6463/aa748a
2. Černák M, Černáková L, Hudec I, Kováčik D, Zahoranová A (2009) EPJ Appl Phys 47(2):22806. https://doi.org/10.1051/epjap/2009131
3. Holländer A, Cosemans P (2020) Plasma Process Polym 17(1):1900155. https://doi.org/10.1002/ppap.201900155
4. Kogelschatz U (2003) Plasma Chem Plasma Process 23(1):1–46. https://doi.org/10.1023/A:1022470901385
5. Galmiz O, Pavliňák D, Zemánek M, Brablec A, Černák M (2017) Plasma Process Polym 14(9):1600220. https://doi.org/10.1002/ppap.201600220
6. Ivanova TV, Krumpolec R, Homola T, Musin E, Baier G, Landfester K, Cameron DC, Černák M (2017) Plasma Process Polym 14(10):1600231. https://doi.org/10.1002/ppap.201600231

7. Alenazi NA, Hussein MA, Alamry KA, Asiri AM (2017) Des Monomers Polym 20(1):532–546. https://doi.org/10.1080/15685551.2017.1398208
8. Zhao C, Xue J, Ran F, Sun S (2013) Prog Mater Sci 58(1):76–150. https://doi.org/10.1016/j.pmatsci.2012.07.002
9. Van der Bruggen B (2009) J Appl Polym Sci 114(1):630–642. https://doi.org/10.1002/app.30578
10. Marjani A, Nakhjiri AT, Adimi M, Jirandehi HF, Shirazian S (2020) Sci Rep 10(1):1–11. https://doi.org/10.1038/s41598-020-58472-y
11. Wang H, Park M, Liang H, Wu S, Lopez IJ, Ji W, Li G, Snyder SA (2017) Water Res 125:42–51. https://doi.org/10.1016/j.watres.2017.08.030
12. Tsehaye MT, Wang J, Zhu J, Velizarov S, Van der Bruggen B (2018) J Memb Sci 550(January):462–469. https://doi.org/10.1016/j.memsci.2018.01.022
13. Ren K, Zhou J, Wu H (2013) Acc Chem Res 46(11):2396–2406. https://doi.org/10.1021/ar300314s
14. Pentecost AM, Martin RS (2015) Anal Methods 7(7):2968–2976. https://doi.org/10.1039/c5ay00197h
15. Chan CY, Goral VN, DeRosa ME, Huang TJ, Yuen PK (2014) Biomicrofluidics 8(4):046505. https://doi.org/10.1063/1.4894409
16. Jullien MC, Pascual M, Kerdraon M, Rezard Q, Jullien MC, Champougny L (2019) Soft Matter 15(45):9253–9260. https://doi.org/10.1039/c9sm01792e
17. Sabatini V, Checchia S, Farina H, Ortenzi MA (2016) Macromol Res 24(9):800–810. https://doi.org/10.1007/s13233-016-4105-6
18. Vrlinič T, Vesel A, Cvelbar U, Krajnc M, Mozetič M (2007) Surf Interface Anal 39(6):476–481. https://doi.org/10.1002/sia.2548
19. Homola T, Wu LYL, Černák M (2014) J Adhes 90(4):296–309. https://doi.org/10.1080/00218464.2013.794110
20. Feng J, Wen G, Huang W, Kang ET, Neoh KG (2006) Polym Degrad Stab 91(1):12–20. https://doi.org/10.1016/j.polymdegradstab.2005.05.001
21. Vesel A, Zaplotnik R, Kovac J, Mozetic M (2018) Plasma Sour Sci Technol 27(9):094005. https://doi.org/10.1088/1361-6595/aad486
22. Gonzalez E, Hicks RF (2010) Langmuir 26(5):3710–3719. https://doi.org/10.1021/la9032018
23. Jokinen V, Suvanto P, Franssila S (2012) Biomicrofluidics 6(1):016501. https://doi.org/10.1063/1.3673251
24. Guimond S, Wertheimer MR (2004) J Appl Polym Sci 94(3):1291–1303. https://doi.org/10.1002/app.21134
25. Strobel M, Dunatov C, Strobel JM, Lyons CS, Perron SJ, Morgen MC (1989) J Adhes Sci Technol 3(1):321–335. https://doi.org/10.1163/156856189X00245
26. Du K, Jiang Y, Huang PS, Ding J, Gao T, Choi CH (2018) J Micromech Microeng 28(1):14006. https://doi.org/10.1088/1361-6439/aa9d28
27. Fernández-Blázquez JP, Del Campo A (2012) Soft Matter 8(8):2503–2508. https://doi.org/10.1039/c2sm06739k
28. Shekargoftar M, Kelar J, Krumpolec R, Jurmanova J, Homola T (2018) IEEE Trans Plasma Sci 46(10):3653–3661. https://doi.org/10.1109/TPS.2018.2861085
29. Šimor M, Ráhel' J, Vojtek P, Černák M, Brablec AA (2002) Appl Phys Lett 81:2716. https://doi.org/10.1063/1.1513185
30. Homola T, Matoušek J, Hergelová B, Kormunda M, Wu LYL, Černák M (2012) Polym Degrad Stab 97(11):2249–2254. https://doi.org/10.1016/j.polymdegradstab.2012.08.001
31. Shekargoftar M, Krumpolec R, Homola T (2018) Mater Sci Semicond Process 75:95–102. https://doi.org/10.1016/j.mssp.2017.11.022
32. Kelar J, Čech J, Slavíček P (2015) Acta Polytech 55(2):109–112. https://doi.org/10.14311/AP.2015.55.0109
33. Grace JM, Gerenser LJ (2003) J Dispers Sci Technol 24(3–4):305–341. https://doi.org/10.1081/DIS-120021793
34. Rezaei F, Dickey MD, Bourham M, Hauser PJ (2017) Surf Coat Technol 309:371–381. https://doi.org/10.1016/j.surfcoat.2016.11.072
35. Gonzalez E, Barankin MD, Guschl PC, Hicks RF (2009) IEEE Trans Plasma Sci 37(6 PART 1):823–831. https://doi.org/10.1109/TPS.2009.2014769
36. Afkham S, Raisi A, Aroujalian A (2016) Desalin. Water Treat 57(56):26976–26992. https://doi.org/10.1080/19443994.2016.1175384
37. Pal S, Ghatak SK, De S, DasGupta S (2008) Appl Surf Sci 255(5 PART 1):2504–2511. https://doi.org/10.1016/j.apsusc.2008.07.184
38. Dong LC, Kim SH, Yang IH, Kim D, Sung YC, Kim BH (2004) Macromol Res 12(6):553–558. https://doi.org/10.1007/bf03218443

39. Vesel A (2010) Surf Coat Technol 205(2):490–497. https://doi.org/10.1016/j.surfcoat.2010.07.016
40. Häidopoulos M, Horgnies M, Mirabella F, Pireaux JJ (2008) Plasma Process. Polym 5(1):67–75. https://doi.org/10.1002/ppap.200700067
41. Bitar R, Asadian M, Van Vrekhem S, Cools P, Declercq H, Morent R, De Geyter N (2018) Surf Coat Technol 350:985–996. https://doi.org/10.1016/j.surfcoat.2018.03.041
42. Olabanji OT, Bradley JW (2012) Plasma Process. Polym 9(9):929–936. https://doi.org/10.1002/ppap.201200011
43. Lawton RA, Price CR, Runge AF, Doherty WJ, Saavedra SS (2005) Colloids Surf Physicochem. Eng Asp 253(1–3):213–215. https://doi.org/10.1016/j.colsurfa.2004.11.010
44. Lim H, Lee Y, Han S, Cho J, Kim J (2001) J Vac Sci Technol A 19:1490. https://doi.org/10.1116/1.1382650
45. Novák I, Florián Š (2004) J Mater Sci 39(6):2033–2036. https://doi.org/10.1023/B:JMSC.0000017765.69441.dd
46. Beamson D, Briggs G (1992) High resolution XPS of organic polymers: the scienta ESCA300 database, 1st edn. Wiley, New York
47. Wohlfart E, Fern Andez-Bl Azquez JP, Knoche E, Bello A, Erez EP, Arzt E, Anzazu Del Campo A (2010) Macromolecules 43:9908–9917. https://doi.org/10.1021/ma101889s
48. Junkar I, Cvelbar U, Vesel A, Hauptman N, Mozetič M (2009) Plasma Process. Polym 6(10):667–675. https://doi.org/10.1002/ppap.200900034